



Landsvirkjun

LV-20 -00

# Seismic Monitoring in Krafla, Námafjall and Þeistareykir

November 2018 to November 2019



# Seismic Monitoring in Krafla, Námafjall and Þeistareykir

November 2018 to November 2019



ÍSOR-2020/003

Project no.: 19-0069

February 2020



## Key Page

LV report no: LV-2020-003

Date: February 2020

Number of pages: 22

Copies: 2

Distribution:

- ☒ On [www.lv.is](http://www.lv.is)  
☒ Open  
☐ Limited until

Title:

Seismic Monitoring in Krafla, Námafjall and Þeistareykir.  
November 2018 to November 2019

Authors/Company:

Hanna Blanck, Þorbjörg Ágústsdóttir, Kristján Ágústsson and Karl Gunnarsson

Project manager:

Ásgrímur Guðmundsson (LV)

Gylfi Páll Hersir (ÍSÖR)

Prepared for:

Prepared by Iceland GeoSurvey (ÍSÖR) for Landsvirkjun.

Co operators:

Abstract:

From November 2018 to October 2019, 3770 earthquakes were located in the greater Krafla area including the Námafjall and Þeistareykir geothermal areas. In Krafla, earthquakes are up to 2.5 km deep while reaching down to about 6 km in Þeistareykir and Námafjall. The magnitude distribution also differs significantly in the three areas from a wide range in Krafla to a higher ratio of bigger magnitudes in Þeistareykir and only small magnitudes in Námafjall. Velocity ratios calculated from Wadati diagrams show decreased values compared to values typically found in the Icelandic crust both in the Krafla and Þeistareykir geothermal areas. In Námafjall the ratio is higher and about the same as typically found in the Icelandic crust.

Re-injection rates in re-injection wells KG-26 and KJ-39 are very stable apart from a few short interruptions. The few interruptions are not followed by noticeable changes in seismicity. The re-injection rate in well KJ-35 is more variable with longer periods without re-injection, but no fluctuation in measured earthquake numbers can be related to changes in re-injection rates. Focal mechanisms of selected earthquakes show that most events occur on normal faults or are a combination of normal and oblique strike-slip faulting. The semi-annual fluctuation pattern of the number of earthquakes is continued.

Keywords:

Krafla, Námafjall, Þeistareykir, seismicity, earthquakes,  
Vp/Vs ratio, b-value, focal mechanism, seasonal variations  
ÍSÖR, Landsvirkjun

ISBN no:

Approved by Landsvirkjun's  
project manager

Project manager's signature



Reviewed by

Egill Árni Guðnason

## Ágrip

Frá nóvember 2018 til október 2019 voru staðsettir 3370 skjálftar á jarðhitasvæðum Kröflu, Námafjalls og Þeistareykja. Dýpstu skjálftarnir í Kröflu mælast á um 2,5 km dýpi en á um 6 km dýpi bæði í Námafjalli og á Þeistareykjum. Stærðardreifing skjálfta er breytileg milli svæða. Mesti breytileikinn fyrirfinnst í Kröflu, hlutfall stórra skjálfta er hæst á Þeistareykjum en einungis litlir skjálftar mælast í Námafjalli. Hraðahlutfall, reiknað út frá Wadati-gröfum, sýnir lægra gildi í Kröflu og á Þeistareykjum en almennt gerist í jarðskorpunni á Íslandi. Í Námafjalli er hlutfallið hinsvegar sambærilegt við það sem almennt gerist.

Niðurdæling í niðurdælingarholurnar KG-26 og KJ-39 var stöðug á þessu tímabili, ef frá eru taldar nokkrar stuttar truflanir. Engin fylgni sést milli breytingar á niðurdælingu og skjálftavirkni. Óregluleg niðurdæling var í holu KJ-35 en hún leiddi heldur ekki til sveiflna í fjölda skjálfta sem mældust. Brotlausnir skjálfta í hæsta gæðaflokki sýna að flestir skjálftanna voru annaðhvort siggengisskjálftar eða blanda sig- og sniðgengis-skjálfta. Árstíðarbundnar sveiflur í skjálftavirkni eru enn til staðar, líkt og fyrri ár.

## Table of contents

<b>1</b>	<b>Introduction .....</b>	<b>7</b>
<b>2</b>	<b>Recorded earthquakes .....</b>	<b>7</b>
<b>3</b>	<b>Spatial distribution of events .....</b>	<b>8</b>
3.1	Krafla .....	9
3.2	Peistareykir .....	9
3.3	Námafjall .....	9
<b>4</b>	<b>Vp/Vs ratio.....</b>	<b>12</b>
<b>5</b>	<b>Injection rate and earthquake activity .....</b>	<b>13</b>
<b>6</b>	<b>Magnitude frequency relation.....</b>	<b>14</b>
6.1	B-value calculations .....	15
<b>7</b>	<b>Focal mechanisms .....</b>	<b>15</b>
<b>8</b>	<b>Semi-annual fluctuations .....</b>	<b>18</b>
<b>9</b>	<b>Summary.....</b>	<b>19</b>
<b>10</b>	<b>References.....</b>	<b>20</b>
	<b>Appendix: Focal mechanism .....</b>	<b>21</b>

## List of figures

Figure 1.	<i>Time-magnitude plot for the events plotted in Figure 2 .....</i>	<i>8</i>
Figure 2.	<i>Spatial and depth distribution of relatively relocated earthquakes in map view and E-W and S-N cross-sections. ....</i>	<i>10</i>
Figure 3.	<i>Map view, N-S and E-W cross-sections and depth distribution of the events relatively relocated in the Peistareykir (a), Krafla (b) and Námafjall (c) geothermal areas..</i>	<i>11</i>
Figure 4.	<i>Vp/Vs ratio calculated for the Krafla, Peistareykir and Námafjall geothermal areas .....</i>	<i>12</i>
Figure 5.	<i>Comparison of re-injection rate and earthquake number for wells KG-26, KJ-35 and KJ-39 as recorded inside the orange, green and red box, respectively.....</i>	<i>14</i>
Figure 6.	<i>Magnitude-frequency relation .....</i>	<i>15</i>
Figure 7.	<i>Focal mechanisms for 35 selected events .....</i>	<i>16</i>
Figure 8.	<i>Graphic summary of all 35 double-couple focal mechanisms located in the Krafla and in Peistareykir geothermal areas .....</i>	<i>17</i>
Figure 9.	<i>Number of daily recorded events in Krafla geothermal area.....</i>	<i>18</i>



# 1 Introduction

This report presents the results of earthquake monitoring in Krafla, Þeistareykir and Námafjall geothermal areas, for the period from November 1<sup>st</sup> 2018 to October 31<sup>st</sup> 2019. The local seismic network is developed and maintained by Iceland GeoSurvey (ÍSOR). Raw data is automatically streamed to ÍSOR, where it is processed and analyzed. The earthquakes presented in this report have been imported into the PETREL software.

The seismic network remains unchanged from last year. For a detailed description of the seismic stations and a map of the network see Blanck et al. (2018).

## 2 Recorded earthquakes

From November 1<sup>st</sup> 2018 until October 31<sup>st</sup> 2019 a total of 3770 earthquakes were detected and located at the geothermal fields of Krafla, Þeistareykir and Námafjall. The national seismic network operated by the IMO located 482 earthquakes in the same area and period. This year over 1000 fewer earthquakes were recorded compared to last year (Blanck et al., 2018). The reason for the decreased number of earthquakes is not thought to be due to less activity but rather due to changes made in the automatic earthquake location procedure. From the summer of 2019, the location criterion was tightened. Now only events that are detected automatically on 10 stations or more are passed to the location stage. Therefore, very small events may be omitted in the automatic procedure. Offline test runs with different location criteria show that the total number has not changed in comparison to the year before. These tests require further investigation in the automatic detection and location procedures at ÍSOR for continued monitoring of the area.

The daily earthquake activity is subject to variations. Periods with an apparent lack of small magnitude earthquakes may indicate bad weather conditions resulting in low signal-to-noise ratio of the recorded seismicity. Since July 2019, there is a decrease in activity which correlates to the change in location procedures. This is illustrated in Figure 1 where we see this decrease both in the number of earthquakes and their cumulative number, which increases less steeply after July 2019. From November 1<sup>st</sup> 2018 until June 30<sup>th</sup> 2019 the average number of earthquakes per day is 12 while from July 1<sup>st</sup> 2019 to October 30<sup>th</sup> 2019 it is significantly lower with 7.1 earthquakes per day. However, this drastic decrease is not seen in the offline test runs as explained above.

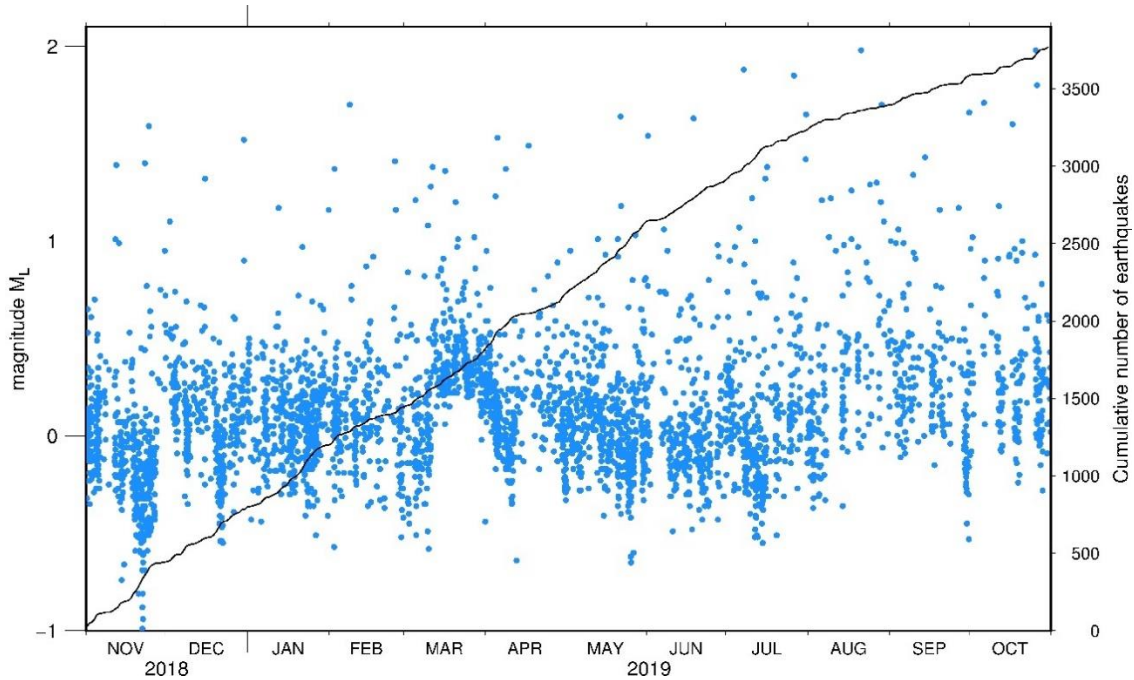


**Figure 1.** Time-magnitude plot for the events plotted in Figure 2. Each located earthquake is represented by a blue dot according to its origin time and magnitude. The activity is characterized by distinct swarms with short quiet periods. The cumulative number of earthquakes (black line) shows a smooth increase with time, indicating long term continuous seismic activity until July 2019 after which less activity is recorded and the slope decreases.

### 3 Spatial distribution of events

For clarity, results are presented for individual areas (Krafla, Námafjall and Þeistareykir) separately (black boxes in Figure 2). In total, 3062 (4293 last year) earthquakes were located in the Krafla geothermal area, 112 (197 last year) in Námafjall and 294 (319 last year) in Þeistareykir (Figure 2). A small number of earthquakes were located outside the defined areas, that is, south of Þeistareykir, north and west of Krafla and between Krafla and Námafjall. All earthquakes were automatically detected and preliminary located using the Seiscomp3 software. The data was then manually repicked and located using the NonLinLoc algorithm (Lomax et al., 2000) and eventually relatively relocated using the hyppDD2.1 software (Waldhauser and Ellsworth, 2000). Both the location and the relative relocation method take the absolute elevation of the seismic stations into account in their location routines. For 3521 out of the total of 3770 earthquakes, relative, high-precision locations could be obtained.

### **3.1 Krafla**

Most earthquakes in the Krafla geothermal area are shallow with hypocentre depths between 0.5 and 2.0 km b.s.l. and the majority is located between 1.0 and 2.0 km depth (Figure 3). The production area is highly seismically active as well as the areas NNE and SSW of Leirhnjúkur. Earthquakes located at the edges of these clusters are deeper, down to ca. 3 km. These active areas are clearly separated by areas of little or no seismicity. It stands out that most of the larger earthquakes ( $M_L > 0.5$ ) are located at the lower edge of the depth range (in about 2 km depth). Since larger earthquakes are recorded on more stations, their hypocenters are expected to be more accurate. Magnitudes ( $M_L$ ) in Krafla vary from -1.16 to 1.98.

### **3.2 Peistareykir**

In Peistareykir there are two distinctly separated clusters, one below the northwestern part of the Bæjarfjall mountain and around it, i.e., below the main production area. Then there is a small cluster about 2 km north of the Bæjarfjall mountain. In the production area, earthquake depth ranges from about 1.5 to 4 km while the northern cluster lies between 4 and 6 km depth. Magnitudes ( $M_L$ ) in Peistareykir vary from -0.37 to 1.80.

### **3.3 Námafjall**

In Námafjall area earthquakes are located in one single vertical cluster with most of the activity located between 2 and 5 km depth. Magnitudes ( $M_L$ ) vary from -0.34 to 1.02.

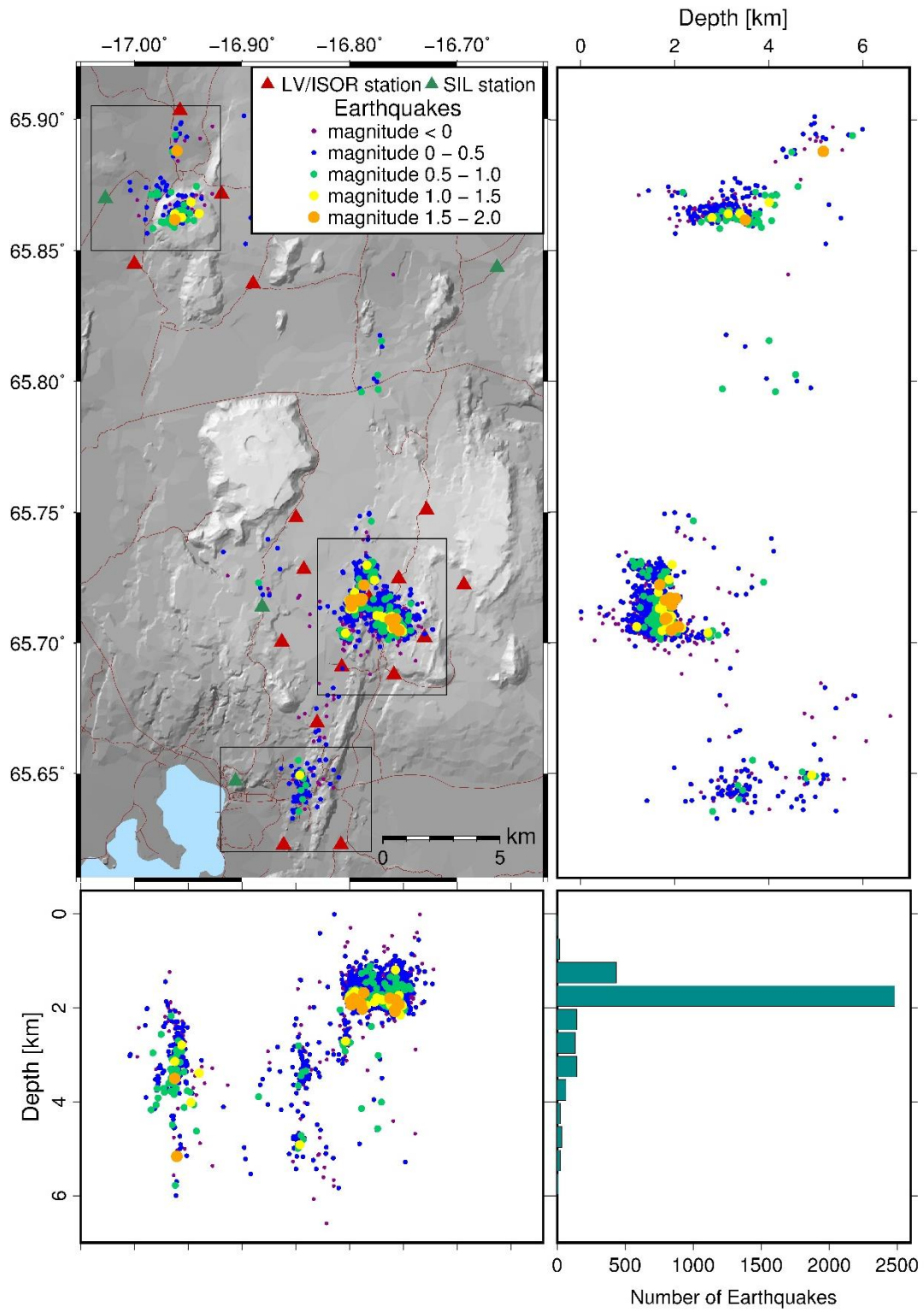


**Figure 2.** Spatial and depth distribution of relatively relocated earthquakes in map view and E-W and S-N cross-sections.

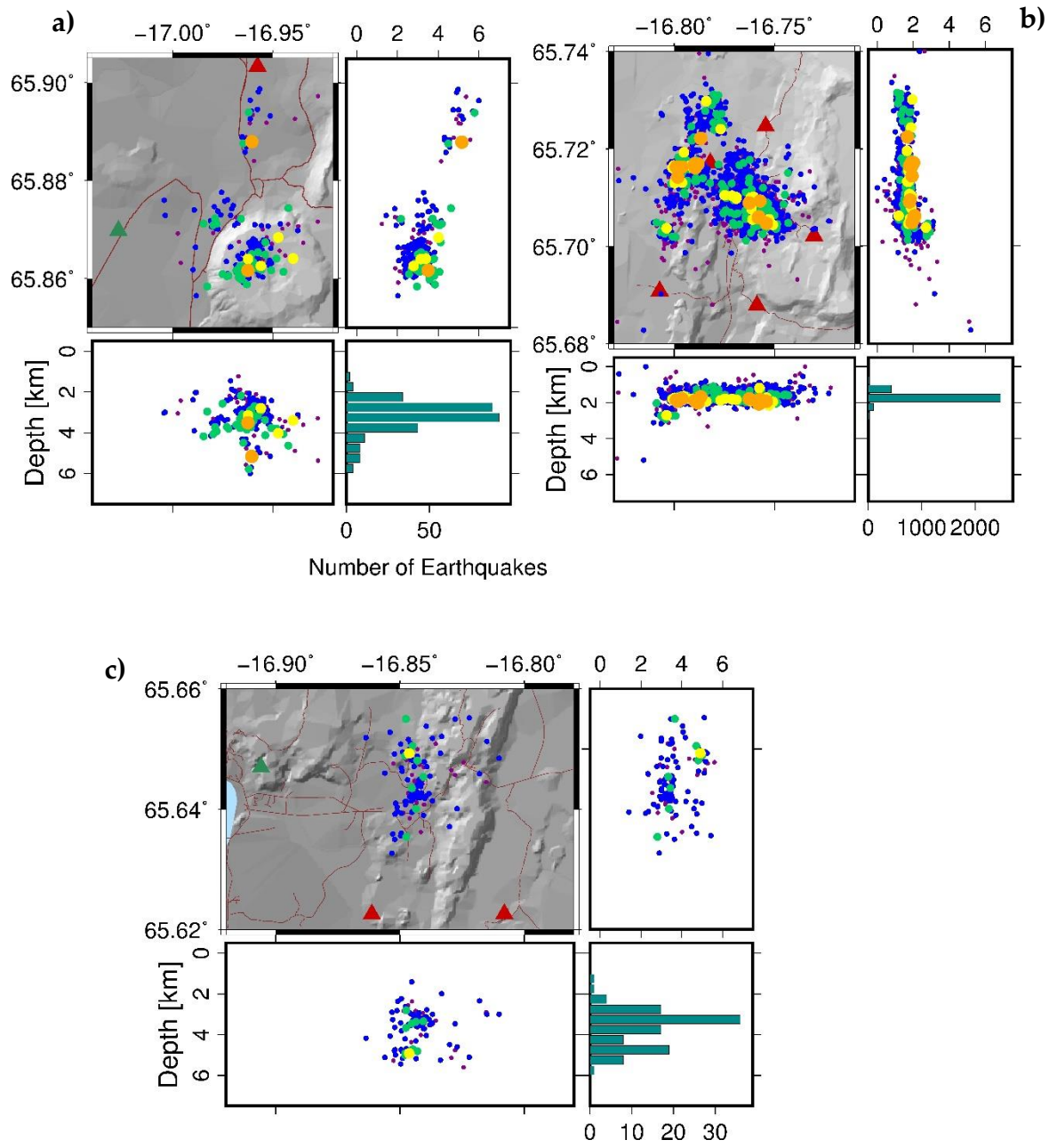


**Figure 3.** Map view, N-S and E-W cross-sections and depth distribution of the events relatively relocated in the Þeistareykir (a), Krafla (b) and Námafjall (c) geothermal areas.

## 4 Vp/Vs ratio

We use standard Wadati diagrams (Wadati, 1933) to estimate Vp/Vs ratios in the Krafla, Þeistareykir and Námafjall geothermal areas. In a Wadati diagram, the difference of the S- and P-wave travel times is plotted as a function of the P-wave travel time. The relationship between the two should be linear and the slope of the best fitting straight line, determined with linear regression, gives a reasonable estimate of the Vp/Vs ratio in the crust (Figure 4). This ratio averages over the whole travel paths of seismic waves for individual earthquakes. To ensure that the calculated Vp/Vs is representative of the crust within each of the areas, only earthquakes and stations from within each of the black boxes (as marked in Figure 1) are used. Changes in the Vp/Vs ratio are associated with the elastic parameters of the crust but also with porosity, pore filling and stress state.

In the Krafla geothermal area, the Vp/Vs ratio derived from the Wadati diagram is  $1.71 \pm 0.01$ , and  $1.74 \pm 0.02$  in Námafjall which is a slight increase compared to last year's result. In Þeistareykir, the ratio derived from this year's data is  $1.76 \pm 0.01$  which is identical to last year's result. The Vp/Vs ratio in Krafla and Þeistareykir are lower than typical values found in the Icelandic crust whereas Námafjall is more aligned with those typical values (Brandsdóttir and Menke, 2008). Low Vp/Vs ratio is generally associated with weaker, more fractured crust.

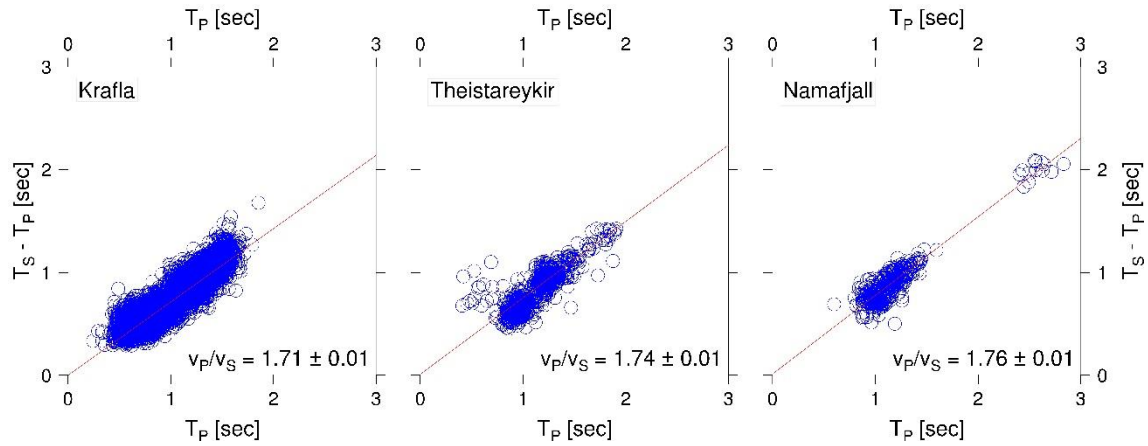


**Figure 4.** Vp/Vs ratio calculated for the Krafla, Þeistareykir and Námafjall geothermal areas. The ratio is lowest in Krafla with 1.71 while it is 1.74 in Þeistareykir and 1.76 in Námafjall.

## 5 Injection rate and earthquake activity

For the period covered in this report, re-injection rate information for three wells was available, that is KG-26, KJ-35 and KJ-39. The re-injection rate data for the three wells came in different format and resolution. For well KG-26, the November and December 2018 data consist of one measurement per day, for 2019 there were recording of the re-injection rate every 5 minutes. For well KJ-35, re-injection rates were recorded 1 to 5 times per day and for well KJ-39, high resolution data recorded every 5 minutes was available. To standardize the data, we calculated the average re-injection rate per day for each well from the available information. To compare the re-injection rate and the numbers of recorded earthquakes we chose a small area around the wells as indicated in Figure 5 (coloured boxes).

KG-26: For most of the time and with few short interruptions the re-injection rate is constant and lies between 70 and 75 l/s. From late June to late September 2019 the re-injection rate is less stable and short-term fluctuation vary from 40 to 75 l/s.

KJ-35: The data available for the re-injection rate in KJ-35 is very variable with peaks of maximum daily average re-injection rates of about 60 l/s while for most of the time no water was injected.

KJ-39: Like in KG-26, the re-injection rate in KJ-39 been almost constant over the study period. The first half of November 2018 the re-injection rate is about 30 l/s, on 15<sup>th</sup> November it is reduced to about 10 l/s and remains constant for the rest of time except for a short interruption at the beginning of June 2019.

The seismicity in geothermal systems often responds very rapidly to changes in both re-injection and production (Cardiff et al., 2018). Therefore, we look at changes in re-injection rate and observe the seismicity in a short time window afterwards. Both in well KG-26 and KJ-39 there are only few of these changes and in both cases a change in seismicity cannot be observed. If there is a variation in activity that can be related to the changes in re-injection rate, it is smaller than the tectonic earthquake fluctuations. In well KJ-35 there are many abrupt changes in the re-injection rate but also here the seismic activity appears to remain unchanged. Based on these observations we cannot identify a relationship between the re-injection rate and the seismicity. A week relationship may perhaps be seen in June 2019 in KJ-39, when re-injection is reduced both in KJ-39 and KG-26 simultaneously. The depth section of Figure 5 shows clearly that the seismicity is concentrated at and around the base level of the boreholes. The seismicity maps the brittle-ductile boundary in about 2 km depth (for detailed analysis see Ágústsson and Blanck (2019)).

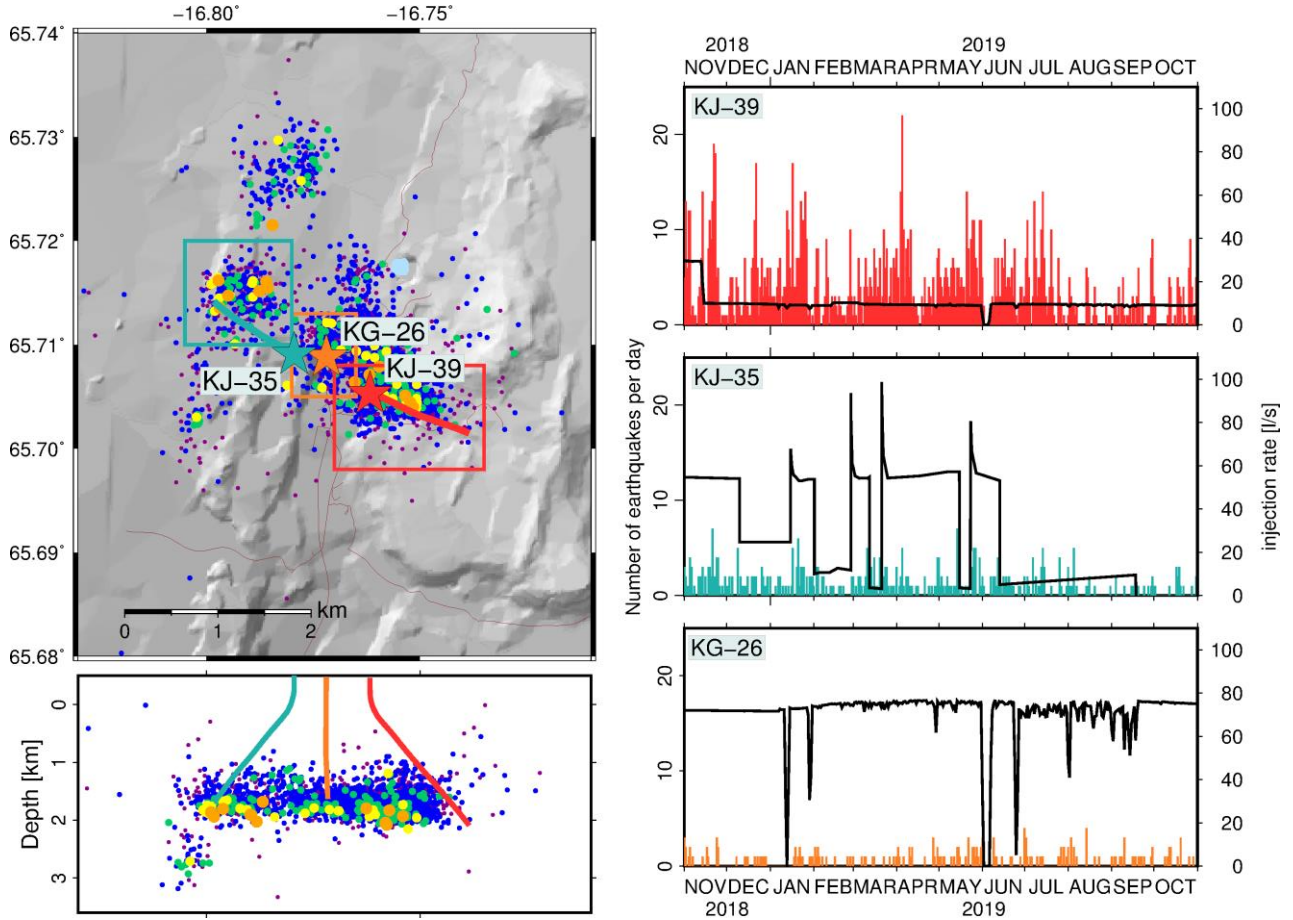


**Figure 5.** Comparison of re-injection rate and earthquake number (right) for wells KG-26, KJ-35 and KJ-39 as recorded inside the orange, green and red box, respectively (left).

## 6 Magnitude frequency relation

Investigating the magnitude distribution provides information on the strength of crust. Magnitudes ( $M_L$ ) in Krafla vary from -1.16 to 1.98. The catalogue is complete down to magnitudes of about 0. In Þeistareykir magnitudes range from -0.37 to 1.80 and in Námajfall from -0.34 to 1.02 while the catalogues are complete down to about magnitude 0.3.

As we have already seen in earlier years, the magnitude distribution varies significantly between the different areas. In Krafla and Þeistareykir, magnitudes reach comparable high values, but the smallest earthquakes that can be recorded are much smaller in Krafla that can probably be ascribed to the sensitivity of networks in the areas, i.e., the station density and network geometry. The magnitude of completion,  $M_c$ , is an indicator of the quality of a dataset. To allow a comparison of different areas or to follow the variations of an active area over time, it is crucial to have a low and consistent  $M_c$ .

## 6.1 B-value calculations

The slope of the cumulative numbers of earthquakes arranged according to magnitude is called the b-value and indicates to which extent a given earthquake distribution is following the Gutenberg-Richter relationship (Gutenberg and Richter, 1956). In the year covered in this report we see a slight variation compared to the year before. In Krafla the b value is 1.5 (1.3 last year), in Þeistareykir it is 1.4 (1.3 last year) and in Námajfall it is 1.9 (2.1 last year). The increase in Krafla and Þeistareykir is probably due to re-evaluation of the magnitude calculation.

All three areas show elevated b-values, indicating limited strength of the crust where stress is released at an early stage as the crust cannot sustain high stresses.

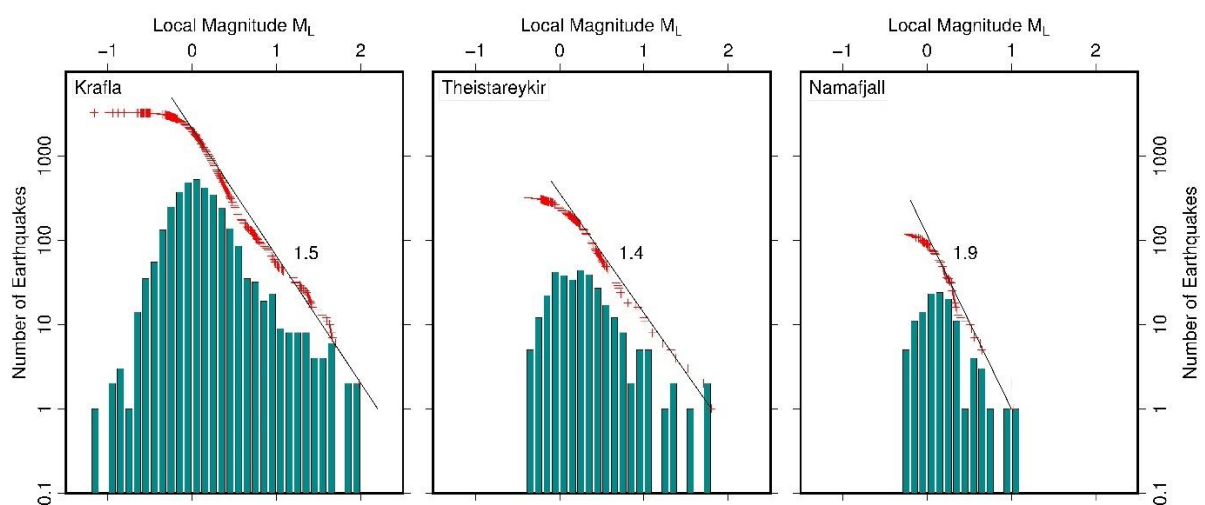


**Figure 6.** Magnitude-frequency relation. Green bars represent the absolute number and the red stars the cumulative number of earthquakes. Black lines approximate the slope of the cumulative number, the b-values are given.

## 7 Focal mechanisms

Focal mechanisms describe the deformation of the crust caused by an earthquake. They are based on the polarities of the first arrivals of the P-wave at all recording seismic stations. The movement pattern provides information about the rupture mechanism and the probable orientation of the stress field in which it occurred. A focal mechanism has two nodal planes but without further information, e.g. geological, it is not possible to distinguish which of the two nodal planes represents the rupture plane of the earthquake.

We use three criteria to select earthquakes for focal mechanism calculation to ensure a sufficient quality of the results; 1) magnitude of  $M_L > 1.0$ ; 2) an azimuth gap of  $< 180^\circ$  and 3) that a minimum of 8 polarities could be identified. 35 earthquakes fulfilled these criteria and focal mechanisms were calculated using both the HASH1.2 (Hardebeck and Shearer, 2002) and the MTFIT software (Pugh and White, 2018). The results from the

MTFIT software showed a much better fit to the data and could resolve focal mechanisms for a larger number of earthquakes. Therefore, in this report, we present the results of this method only. In Krafla geothermal area were 29 of the 35 earthquakes located in and the remaining 6 in Þeistareykir. In Þeistareykir, there are two normal faulting earthquakes, two intermediate ones (oblique strike-slip) and the only strike-slip event. In Krafla, most events are on normal or intermediate faults (oblique strike-slip), but also two thrust faults could be identified.

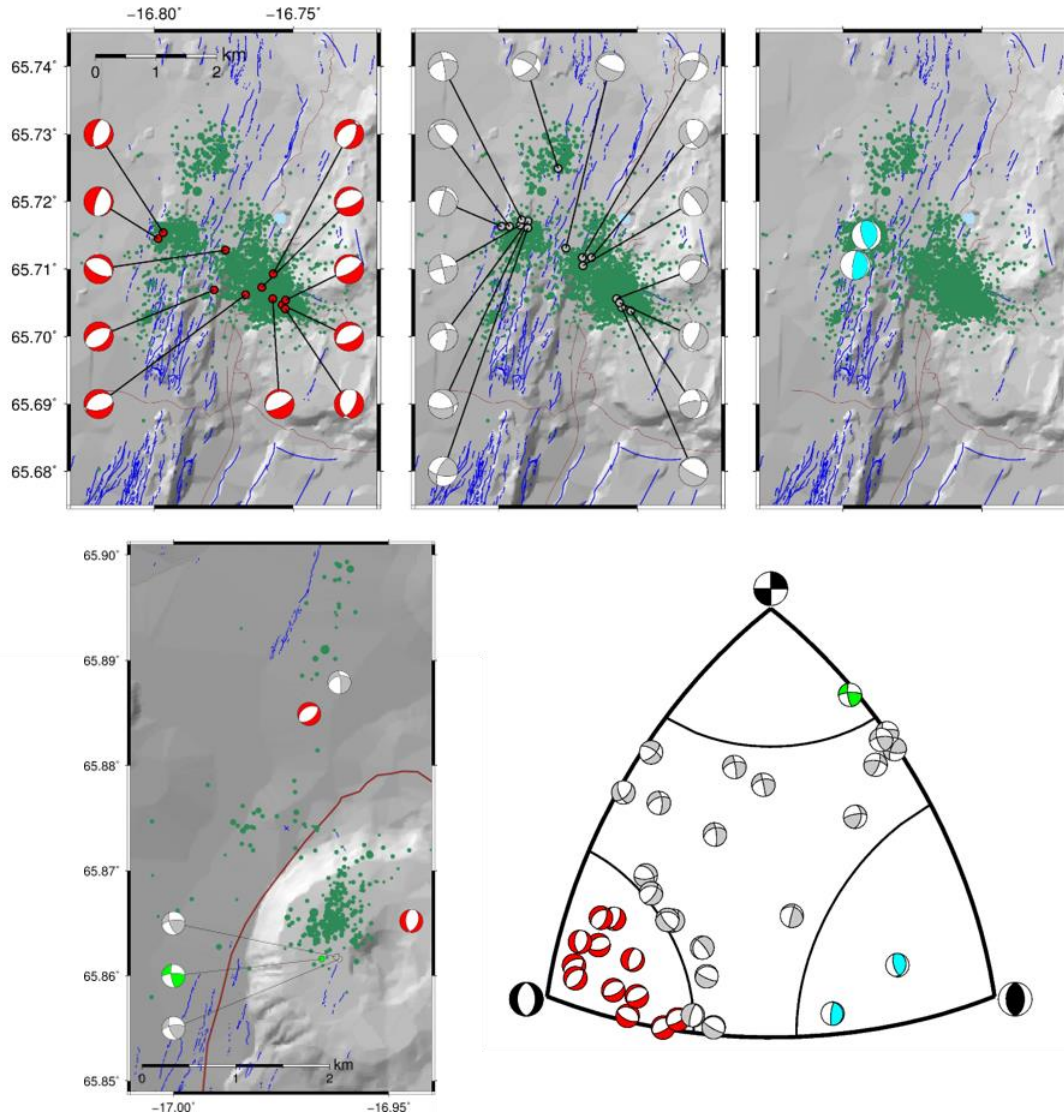


**Figure 7.** Focal mechanisms for 35 selected events. These are lower hemisphere plots and the compressional quadrants are coloured. The earthquakes in Þeistareykir (bottom left) are at 3.4 to 5.2 km depth b.s.l. while the earthquakes in Krafla (right) lie from 1.7 to 2.1 km depth b.s.l. Mapped surface fractures are plotted in blue. Fractures in Krafla are taken from Hjartardóttir et al. (2016), fractures in Þeistareykir from Magnúsdóttir and Brandsdóttir (2011). Green dots are earthquake location, the same as in Figure 3, dot size scaled by magnitude. The categorization method by Frohlich (1992) was used to further classify the focal mechanisms.

The focal mechanisms show a large variety of fault plane orientations, but some patterns are recognizable in the normal fault mechanisms that show either an E-W or a NW-SE orientation. The majority of the intermediate, the strike-slip and the thrust fault have a similar strike to their respective fissure-swarm, striking NE-SW. For a detailed description of the focal mechanisms, see Table 1 in the Appendix.

We compare the orientations of the nodal planes, that is the two potential rupture planes, to faults that were observed in televiwer imaging of the directionally drilled production well K-41 in the Krafla geothermal area (Árnadóttir et al., 2019). These faults most often strike in firstly NNE-SSW and secondly NNW-SSE direction. The nodal planes of the focal mechanisms we obtained in Krafla show a wide variety and no dominant strike direction can be identified (Figure 8). If we assume that the nodal plane aligned with the fissure swarm is the fault plane, a weak relationship can be found between the focal mechanisms and the televiwer fracture orientation. However, a more detailed study of earthquake source mechanisms, investigating a wider magnitude range of earthquakes, is needed to compare with televiwer and surface faulting.

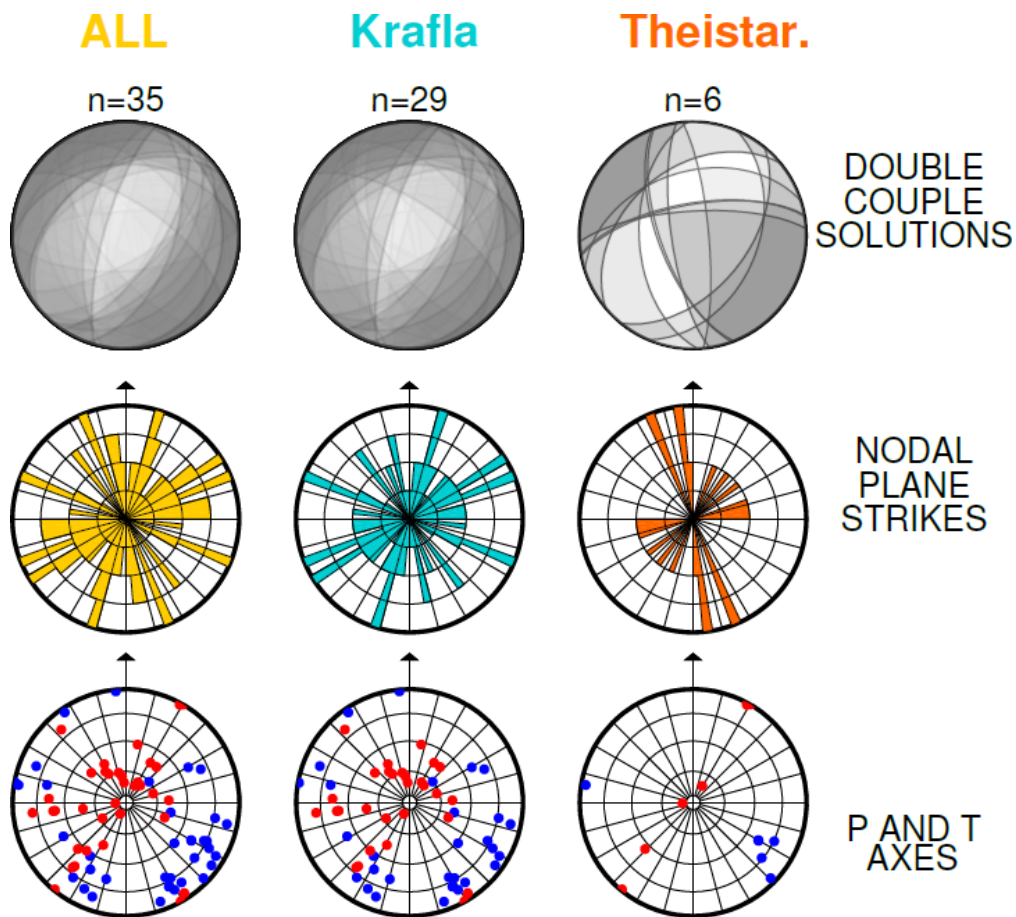


**Figure 8.** Graphic summary of all 35 double-couple focal mechanisms located in the Krafla and in Þeistareykir geothermal areas. The top row shows all focal mechanisms, the middle row shows the orientations of the strikes of the nodal planes and the bottom row shows the orientation of the maximum compressive (P axis, red dots) and minimum compressive stress (T axis, blue dots)

## 8 Semi-annual fluctuations

In previous annual reports we have looked at the number of recorded earthquakes over time and the distribution gave rise to the suspicion that the number of earthquakes is subject to regular variations of about 6-month wavelength. The data from this year has been added to the time-series and lowpass filtered to eliminate outliers (Figure 8). To exclude effects due to the reduced number caused by the change in detection algorithm, we re-count the number of earthquakes per day including only events with a magnitude greater than 0.0, since the magnitude frequency relation suggests that this is the magnitude of completeness of the data set. This newest addition to the timeseries also shows the same fluctuation supporting the six-month regularity hypothesis.

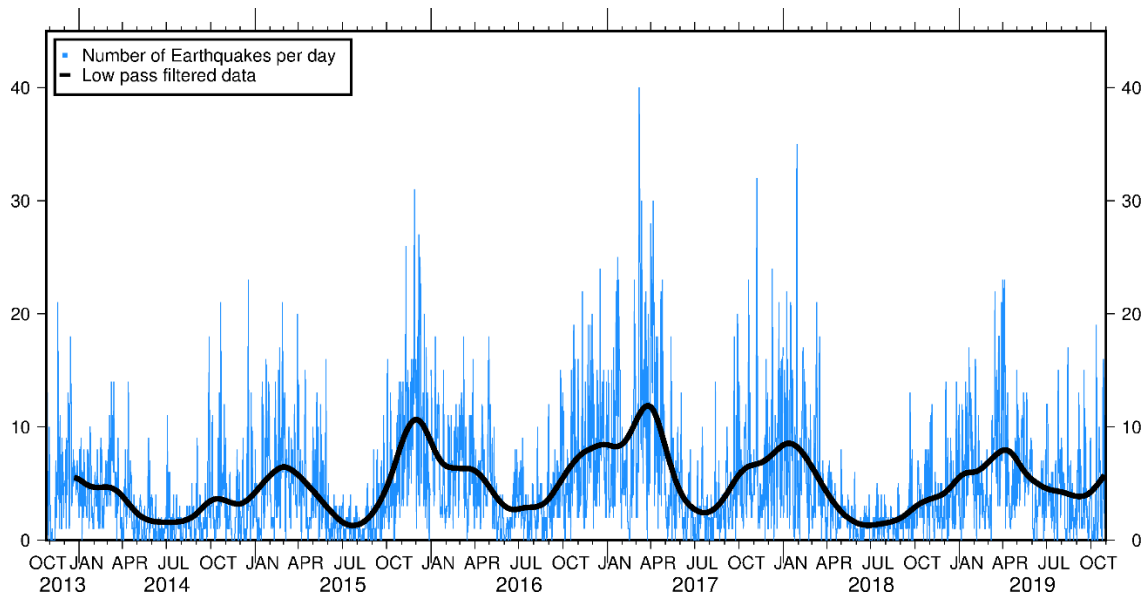


**Figure 9.** Number of daily recorded events in Krafla geothermal area with magnitude ( $M_L$ ) greater than 0.0, from October 25<sup>th</sup> 2013 until October 31<sup>st</sup> 2019 (blue curve) and low pass filtered (black curve).

## 9 Summary
















- From November 1<sup>st</sup> 2018 until October 30<sup>th</sup> 2019 3770 earthquakes were detected and located in Krafla, Þeistareykir and Námafjall geothermal areas. Most earthquakes are located in Krafla, much fewer in Þeistareykir and Námafjall. Depth distribution and magnitude range varies between areas. In Krafla the brittle-ductile boundary is distinct, and the magnitude range is wider than in the other areas.
- $V_p/V_s$  ratios in Krafla, Þeistareykir and Námafjall are 1.71, 1.74 and 1.76, respectively. While the crust in Námafjall has the same value as typically found in the Icelandic crust, the values in Krafla and Þeistareykir are reduced and (within the error) in agreement with what has been seen in these areas in the previous years.
- Changes in the re-injection rate do not clearly correlate to seismicity rates.
- The magnitudes ( $M_L$ ) of the recorded earthquakes in the three geothermal areas differ in range and calculated b-values. Þeistareykir and Námafjall are lacking very small earthquakes, possibly due to the less sensitive networks.
- Focal mechanisms were calculated for 35 selected earthquakes, 29 of which were in Krafla and 6 in Þeistareykir. Most earthquakes are dominated by normal faulting or are a combination of normal and oblique strike-slip faulting. The nodal planes do not show dominant strike directions compared to the televiewer data from well K-41 in Krafla.
- The semi-annual fluctuations in the daily number of earthquakes continue and are comparable to previous years.

















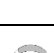

## 10 References

- Ágústsson, K., and Blanck, H. (2019). *Krafla – Jarðskjálftar og niðurdæling*, Iceland GeoSurvey, ÍSOR-2019/022.
- Árnadóttir, S., Ingólfsson, H., Stefánsson, H. Ö., Ingimarsson, H., Tryggvason, H., Egilson, P., Gunnarsson, B. S. and Blischke, A. (2019). *Krafla - Well K-41. Results of Televiewer Imaging at the Krafla Geothermal Field, NE-Iceland*. Iceland GeoSurvey, ÍSOR-2019/075.
- Blanck, H., Ágústsson, K. and Gunnarsson, K. (2018). *Seismic Monitoring in Krafla, November 2017 to November 2018*. Iceland GeoSurvey, ÍSOR-2018/087.
- Brandsdóttir, B., and Menke, W. (2008). The seismic structure of Iceland, *Jökull*, 58, 17–34.
- Cardiff, M., Lim, D. D., Patterson, J. R., Akerley, J., Spielman, P., Lopeman, J., Walsh, P., Singh, A., Foxall, W., Wang, H. F., Lord, N. E., Thurber, C. H., Fratta, D., Mellors, R. J., Davatzes, N. C. and Feigl, K. L. (2018). Geothermal production and reduced seismicity: Correlation and proposed mechanism. *Earth and Planetary Science Letters*, 482, 470-477.
- Frohlich, C. (1992). Triangle diagrams: ternary graphs to display similarity and diversity of earthquake focal mechanisms, *Physics of the Earth and Planetary Interiors*, 75, 193-198.
- Gutenberg, B. and Richter, C. F. (1956). Magnitude and Energy of Earthquakes. *Annali di Geofisica*, 9, 1–15.
- Hardebeck, J.L. and Shearer, P.M. (2002). A new method for determining first-motion focal mechanisms, *Bulletin of the Seismological Society of America* 92, 2264-2276.
- Hjartardóttir, Á. R., Einarsson, P., Magnúsdóttir, S., Björnsdóttir, P. and Brandsdóttir, B. (2016). Fracture systems of the Northern Volcanic Rift Zone, Iceland: an onshore part of the Mid-Atlantic plate boundary, *Geological Society, London, Special Publications*, 420(1), 297-314.
- Lomax, A., Virieux, J., Volant, P. and Berge-Thierry, C. (2000). Probabilistic earthquake location in 3D and layered models, In *Advances in seismic event location* (101-134), Springer, Dordrecht.
- Magnúsdóttir, S. and Brandsdóttir, B. (2011). Tectonics of the Þeistareykir fissure swarm. *Jökull*, 61, 65-79.
- Pugh, D. J. and White, R. S. (2018). MTfit: A Bayesian approach to seismic moment tensor inversion, *Seismological Research Letters*, 89(4), 1507-1513.
- Wadati, K. (1933). On travel time of earthquake waves. *Geophys. Mag.* 7, 101–111.
- Waldhauser, F. and Ellsworth, W.L. (2000). A double-difference earthquake location algorithm: Method and application to the northern Hayworth fault, California, *Bulletin of the Seismological Society of America* 90, 1353-1368.

## Appendix: Focal mechanism

**Table 1.** Details for selected events and their focal mechanism. Locations are calculated using the NLLC algorithm.

	date	time	lat [°]	lon [°]	Depth [km]	M <sub>L</sub>	number of polarities	faulting mechanism	
1	2018-11-12	09:12:48.5 3	65.7165	-16.7922	1.796	1.39	12		intermediate
2	2018-11-23	06:11:27.1 1	65.7038	-16.7525	1.733	1.40	16		intermediate
3	2018-11-24	17:40:33.2 0	65.7161	-16.7895	1.910	1.59	8		intermediate
4	2018-12-15	22:55:68.7 2	65.8616	-16.9615	3.451	1.30	15		intermediate
5	2018-12-30	16:05:24.9 0	65.8616	-16.9656	3.706	1.51	17		strike-slip
6	2019-02-03	00:12:33.5 8	65.7131	-16.7758	1.840	1.36	13		intermediate
7	2019-02-08	17:24:40.4 3	65.7171	-16.7894	2.011	1.71	11		intermediate
8	2019-02-25	20:02:84.0 6	65.7054	-16.7528	2.004	1.42	11		normal
9	2019-03-05	13:49:31.5 7	65.7154	-16.7968	1.702	1.21	11		normal
10	2019-03-11	08:35:21.2 3	65.7150	-16.7915	1.803	1.29	10		thrust
11	2019-03-12	02:01:23.0 8	65.7041	-16.7529	2.011	1.42	11		normal
12	2019-03-20	18:27:23.3 1	65.7128	-16.7744	1.877	1.18	12		normal
13	2019-04-04	22:00:19.7 4	65.7173	-16.7917	1.924	1.21	12		intermediate
14	2019-04-05	15:39:14.8 5	65.7062	-16.7672	1.924	1.53	15		normal
15	2019-04-08	17:58:36.9 6	65.7050	-16.7565	1.904	1.35	13		intermediate
16	2019-04-17	10:02:34.3 2	65.7117	-16.7666	1.780	1.49	14		intermediate
17	2019-05-22	04:17:18.7 8	65.7163	-16.7989	1.863	1.64	16		intermediate

18	2019-06-01	12:59:05.7 3	65.7117	-16.7699	1.635	1.54	16		intermediate
19	2019-06-18	19:36:63.0 5	65.7047	-16.7540	1.931	1.63	15		normal
20	2019-07-07	19:52:26.4 2	65.7145	-16.7986	1.904	1.88	12		intermediate
21	2019-07-10	22:47:47.5 1	65.7249	-16.7786	1.729	1.36	12		intermediate
22	2019-07-15	23:20:10.2 9	65.7043	-16.7557	1.951	1.32	13		intermediate
23	2019-07-16	15:41:83.7 7	65.8652	-16.9448	3.955	1.35	13		normal
24	2019-07-26	18:48:60.4 4	65.7056	-16.7576	2.058	1.85	13		intermediate
25	2019-07-31	06:04:24.0 7	65.7106	-16.7956	1.823	1.42	10		thrust
26	2019-07-31	09:13:15.5 9	65.7170	-16.7897	1.924	1.65	11		intermediate
27	2019-08-06	08:51:33.3 2	65.7069	-16.7785	1.880	1.20	8		normal
28	2019-08-09	17:46:47.3 1	65.8849	-16.9685	5.190	1.21	11		normal
29	2019-08-21	05:27:24.1 5	65.7056	-16.7574	2.045	1.98	12		normal
30	2019-09-09	21:56:21.2 8	65.7105	-16.7697	1.890	1.34	12		intermediate
31	2019-09-14	10:39:38.9 9	65.7073	-16.7613	1.897	1.42	11		normal
32	2019-10-01	02:46:51.8 1	65.7093	-16.7572	1.830	1.66	8		normal
33	2019-10-06	17:05:43.5 6	65.8618	-16.9622	3.498	1.73	16		intermediate
34	2019-10-17	11:52:29.4 9	65.7163	-16.7961	1.803	1.60	8		intermediate
35	2019-10-26	19:23:27.5 4	65.8879	-16.9615	5.163	1.82	15		intermediate